Immunity, Vol. 23, 249–262, September, 2005, Copyright ©2005 by Elsevier Inc. DOI 10.1016/j.immuni.2005.08.001

Perforin Triggers a Plasma Membrane-Repair Response that Facilitates CTL Induction of Apoptosis

Dennis Keefe,[1,2] Lianfa Shi,[1,2] Stefan Feske,[1,3] Ramiro Massol,[1,4] Francisco Navarro,[1,2] Tomas Kirchhausen,[1,4] and Judy Lieberman[1,2,*]
[1]The CBR Institute for Biomedical Research
Boston, Massachusetts 02115
[2]Department of Pediatrics
[3]Department of Pathology
[4]Department of Cell Biology
Harvard Medical School
Boston, Massachusetts 02115

Summary

Perforin delivers granzymes to induce target-cell apoptosis. At high concentrations, perforin multimerizes in the plasma membrane to form pores. However, whether granzymes enter target cells via membrane pores is uncertain. Here we find that perforin at physiologically relevant concentrations and during cell-mediated lysis creates pores in the target-cell membrane, transiently allowing Ca^{2+} and small dyes into the cell. The Ca^{2+} flux triggers a wounded membrane-repair response in which internal vesicles, including lysosomes and endosomes, donate their membranes to reseal the damaged membrane. Perforin also triggers the rapid endocytosis of granzymes into large EEA-1-staining vesicles. The restoration of target-cell membrane integrity by triggering the repair response is necessary for target cells subjected to cytotoxic T lymphocyte attack to avoid necrosis and undergo the slower process of programmed cell death. Thus, the target cell actively participates in determining its own fate during cell-mediated death.

Introduction

Perforin (PFN) plays an essential role in the granule exocytosis pathway of target-cell apoptosis, the main way cytotoxic T cells (CTL) and natural killer (NK) cells eliminate virus-infected cells and tumors. Apoptotic target-cell death is triggered by release of cytotoxic granule contents into the immunological synapse formed by CTL binding to its target cell (Stinchcombe et al., 2001). Cytotoxic granules contain PFN and a group of serine proteases called granzymes (Gzm) in a proteoglycan matrix (Lieberman, 2003). PFN delivers Gzms into the target-cell cytosol. Because multiple Gzms can independently trigger target-cell apoptosis, targeted disruption of any one Gzm gene in mice only modestly affects immune protection. However, there is only one known delivery molecule. Consequently, mice deficient in PFN are profoundly immunodeficient and are unable to protect themselves against viral infection and tumors (Kagi et al., 1994). Humans with familial hemophagocytic lymphohistiocytosis due to PFN gene mutations also have compromised antiviral immunity (Stepp et al., 1999). Although PFN was identified almost 20 years ago and cloned shortly thereafter, the molecular and cellular basis for PFN activity remains uncertain (Catalfamo and Henkart, 2003).

At low "sublytic" concentrations, PFN delivers Gzms to induce apoptosis but causes little cell death on its own. At higher "lytic" concentrations, PFN induces necrotic death, but not apoptosis, independently of granzymes. Apoptosis, which requires activating a series of endogenous pathways, occurs slowly over more than an hour, while necrotic death via PFN occurs within minutes and preempts the ability to undergo programmed cell death. PFN-induced necrosis is thought to be due to loss of plasma membrane integrity. Since CTL and NK cells kill target cells by apoptosis (Russell et al., 1980), sublytic concentrations are thought to be physiologically relevant. The sublytic PFN concentration that induces 5%–15% necrosis delivers Gzms but varies between target cells and preparations and must be carefully titrated for each experiment (Shi et al., 1992).

PFN shares homology with terminal complement components. Because, like complement, PFN multimerizes in membranes to form pores, PFN was originally hypothesized to deliver Gzms to target cells through plasma membrane pores (Masson and Tschopp, 1985; Podack et al., 1985; Sauer et al., 1991; Tschopp et al., 1986; Young et al., 1986). However, PFN pores seen on electron micrographs may be too small ($\leq$50 nm diameter) to act as channels for globular molecules like Gzms. Moreover, at sublytic concentrations, even much smaller molecules, such as trypan blue or propidium iodide (PI), do not diffuse into the cytoplasm of all but a minority of cells (Kawasaki et al., 2000; Metkar et al., 2002).

The plasma membrane-pore model was questioned when GzmB was shown to be endocytosed without PFN (Froelich et al., 1996; Motyka et al., 2000; Pinkoski et al., 1998; Shi et al., 1997; Trapani et al., 2003). Although apoptosis is not induced until PFN is added, initial experiments suggested that apoptosis could be triggered when PFN is added to cells that had previously endocytosed GzmB (Froelich et al., 1996; Pinkoski et al., 1998). This result led to a revised model in which PFN acts to release Gzms from endosomes (Froelich et al., 1996). This idea was supported by finding that adenovirus and bacterial pore-forming proteins, such as streptolysin, that cause endosomal disruption can substitute for PFN to introduce Gzms into target cells (Browne et al., 1999; Froelich et al., 1996; Pinkoski et al., 1998).

How extracellular PFN acting on the plasma membrane could target Gzm release from membrane bound intracellular vesicles was unclear. This caused us to reexamine whether adding PFN to cells, which had previously endocytosed GzmB, could trigger apoptosis. Because the Gzms are highly basic (pIs ~9–11) and the plasma membrane negatively charged, GzmB remains bound to the surface of washed cells, unless cells are washed with high-ionic-strength buffers (Shi et al., 2005). By carefully removing all surface bound GzmB,

*Correspondence: lieberman@cbr.med.harvard.edu

we found that PFN cannot effectively deliver previously endocytosed Gzms. PFN and GzmB must be coendocytosed to release GzmB into the cytosol and trigger apoptosis.

To begin to understand the molecular basis of PFN action, we looked at the effect of sublytic and lytic concentrations of PFN on cell membranes. At sublytic concentrations, PFN damages the plasma membrane to trigger a transient Ca^{2+} flux. Cells need to be able to repair plasma membrane damage that occurs constantly from in vivo mechanical stress. Because cytosolic Ca^{2+} is normally low, while the extracellular milieu is rich in Ca^{2+}, a rise in cytosolic Ca^{2+} above ~100 μM triggers a stereotypic, ubiquitous, and rapid damaged membrane response, sometimes called the "cellular wound-healing response" because it is activated by mechanical trauma to the plasma membrane (McNeil and Steinhardt, 2003). Intracellular vesicles, including endosomes, lysosomes, and multivesicular bodies, are mobilized within seconds to donate their membranes to reseal the damaged plasma membrane (Bi et al., 1995; McNeil and Steinhardt, 2003; Miyake and McNeil, 1995; Reddy et al., 2001; Steinhardt et al., 1994). Cellular wound healing can be detected by finding lysosomal lumenal membrane proteins, such as CD107a (Lamp-1), on the cell membrane.

We find that sublytic PFN triggers a rapid damaged membrane response, which restores plasma membrane integrity to allow codelivered Gzms to induce the slow process of apoptosis. When the repair response is inhibited, cells treated with GzmB and sublytic PFN are more likely to die by necrosis than by apoptosis. GzmB and sublytic PFN treatment is only a model for what happens during granule-mediated cell death by killer lymphocytes. Therefore, we were careful to validate our results using CTL effector cells. Target cells subjected to CTL attack behave like targets treated with GzmB and sublytic PFN. They experience a transient Ca^{2+} flux and respond to repair the damaged membrane by mobilizing intracellular vesicles. Interfering with the repair response also shifts the balance of target-cell death from apoptosis toward necrosis during CTL attack.

Results

A Narrow Window for Perforin Delivery of Granzymes to Induce Apoptosis

U937 cells were treated with native PFN, purified from rat NK cells as described (Shi et al., 2000). At PFN concentrations above 250 ng/ml, a substantial proportion of U937 cells take up trypan blue, but their nuclei do not show morphological features of apoptosis (Figure 1A, data not shown). If GzmB is added with high concentrations of PFN, cells still die mostly by necrosis. This PFN concentration is termed lytic. If the PFN concentration is reduced by half to 125 ng/ml, only 9% of cells take up trypan blue; but if GzmB is added simultaneously, 82% of cells become apoptotic. This PFN concentration, which delivers Gzms but does not cause cell death on its own, is called sublytic. If the PFN concentration is again reduced by half, PFN no longer effectively delivers Gzms. Similar results are obtained with other cells, including K562, HeLa, COS, and B-LCL. The sublytic concentration is between 50 and 500 ng/ml, but the concentration varies from cell to cell and perforin preparation. There is only a 3- to 4-fold variation between a PFN concentration too low to deliver Gzms and a lytic concentration that induces necrosis, with the sublytic concentration somewhere in between. Therefore, we have independently determined the sublytic concentration for each experiment as that inducing 5%–15% trypan blue inclusion in the absence of added Gzms. By contrast to the narrow window for PFN sublytic activity, the dose-response curve for GzmB-induced apoptosis at a fixed sublytic PFN concentration increases steadily from no activity at ~0.25 μg/ml to reach a plateau at ~2 μg/ml (data not shown).

Perforin Perturbs the Plasma Membrane

Within seconds of adding sublytic PFN to HeLa cells, the cell membrane is perturbed with a bubbling appearance caused by the formation of rounded membrane protuberances that enlarge and fuse over the first few minutes (see Movie S1 in the Supplemental Data available online with this article). Blebs of up to 3 μm diameter form focally along the outer membrane. Some blebs resolve over the 10 min of observation and appear to be taken up into the cell. In some cells, tubulations that connect neighboring cells appear. To visualize the membrane better, HeLa cells were labeled with the vital membrane dye DiI and treated with PFN in the presence of the cell impermeant nuclear dye Sytox green (Figure 1B). Sytox green nuclear staining correlates with trypan blue uptake (data not shown) and indicates loss of membrane integrity and necrotic death. Using a sublytic PFN concentration, DiI-staining membrane blebs can be readily seen, but the nuclear dye is largely excluded. A three-dimensional reconstruction of the PFN-treated cell shows multiple membrane-delimited blebs. One of these blebs contains Sytox green, suggesting that the membrane may have been temporarily damaged to allow the dye in, but then resealed (see below; Movie S2). Some of the blebs detach from the cell (Figure 1C). Interestingly, after PFN treatment, DiI also appears to stain intracellular membranes, consistent with a previous report of plasma membrane exchange induced by PFN (Kawasaki et al., 2000). When a lytic concentration of PFN is used, blebs still form, but the membrane barrier is not preserved, allowing Sytox green into the cell.

Sublytic Perforin Triggers a Transient Ca^{2+} Flux in Target Cells

Because a rapid Ca^{2+} flux has been reported in target cells subjected to CTL attack (Poenie et al., 1987) or treated with purified PFN (Binah et al., 1997) and because of the membrane perturbations we observed, we looked at whether sublytic PFN doses induce a Ca^{2+} flux. PFN was added at varying concentrations to HeLa cells preloaded with the Ca^{2+} indicator fura-2. HeLa cells require a higher sublytic concentration of PFN than U937 cells. At 200 ng/ml, a concentration below the sublytic dose (no PI incorporation and no GzmB delivery to induce apoptosis [data not shown]), PFN triggers no Ca^{2+} influx (Figure 2A). At 320 ng/ml, a sublytic concentration at which 9% of cells incorporate

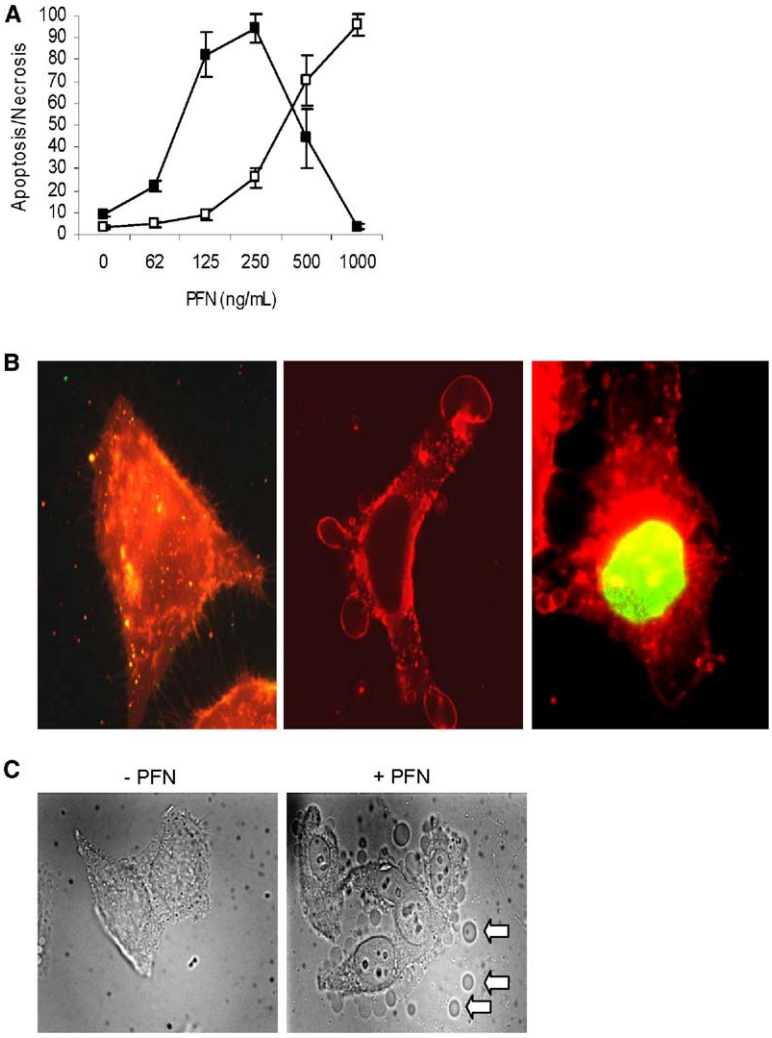

Figure 1. PFN Has a Narrow Window for Delivering GzmB to Induce Apoptosis and Induces Membrane Perturbations at Sublytic Concentrations

(A) U937 cells were treated with PFN alone and assayed for necrosis by trypan blue incorporation (open square) or treated with PFN and GzmB and assayed for apoptosis by nuclear morphology after DAPI staining (closed square). At sublytic concentrations, PFN induces little cell death on its own, but delivers GzmB to induce apoptosis; at lytic concentrations, PFN induces necrosis and adding GzmB does not lead to apoptosis. The range of PFN concentration effective at delivering Gzms to induce apoptosis in U937 cells is narrow (>62 ng/ml, <250 ng/ml).

(B) Sublytic PFN induces focal membrane perturbations, but does not allow dissemination of small dyes like Sytox green. Fluorescence microscopy images of HeLa cells labeled with a fluorescent membrane dye (DiI, red) and treated with buffer alone (left), sublytic PFN (middle), and lytic PFN (right). Plasma membrane integrity was assessed by including the cell impermeant nuclear stain Sytox green in the assay buffer. A single optical section from a Z stack series is depicted. The three-dimensional Z stack is shown in Movie S2.

(C) Some membrane blebs (arrows) detach within minutes of PFN treatment.

PI and PFN delivers GzmB, a transient Ca^{2+} flux lasting ~20–200 s was detected in almost all cells, although the amount of flux was variable (Figure 2B, Movie S3). On video images, Ca^{2+} fluxes were unsynchronized and in some cases appear to be transmitted from one cell to another, possibly via the intercellular bridges seen in Movie S1. At the lytic concentration of 600 ng/ml, PFN caused a sustained increase in intracellular Ca^{2+}, presumably due to irreparable damage, as 38% of cells took up PI (Figure 2C, Movie S4). The increase in intracellular free Ca^{2+} at the lytic dose resolved in most cells only when Ca^{2+} was removed from the perfusing medium. Therefore, the generation and duration of an intracellular Ca^{2+} flux correlates with PFN function along its steep dose-response curve—there is no Ca^{2+} flux below the sublytic concentration, a transient flux at sublytic concentrations, and a sustained flux at lytic concentrations. The transient flux at sublytic PFN concentrations suggests that the plasma membrane was damaged and then could be repaired to restore membrane integrity to exclude extracellular Ca^{2+} only at sublytic concentrations. The Ca^{2+} flux upon PFN treatment was also verified by flow cytometry analysis of fluo-3-AM-loaded U937 cells (Figure 2D). Cells analyzed immediately after exposure to PFN demonstrated increased intracellular Ca^{2+} by mean fluorescence intensity (MFI) as the PFN concentration changed from sublytic to lytic.

Small Molecular Dyes Enter Perforin-Treated Cells, but Are Contained in Membrane-Proximal Blebs

Because of the pore-forming properties of PFN, the most likely explanation for the Ca^{2+} flux in PFN-treated cells is pore formation at the plasma membrane, allowing extracellular Ca^{2+} to enter the Ca^{2+}-poor cytosol. This hypothesis cannot be tested directly by removing or chelating extracellular Ca^{2+} because PFN is inactive in the absence of Ca^{2+}. However, plasma membrane pores might allow small molecule dyes to enter the cell. In fact, when cells are treated with sublytic PFN in medium containing trypan blue, uptake of a small amount of trypan blue into the perturbed membrane bulges is seen, suggesting a breach in the plasma membrane (Figure 3A, U937 cells; Figure 3B, HeLa cells). However, uptake is limited to the blebs and is difficult to see, suggesting that it is transient. The dye does not dis-

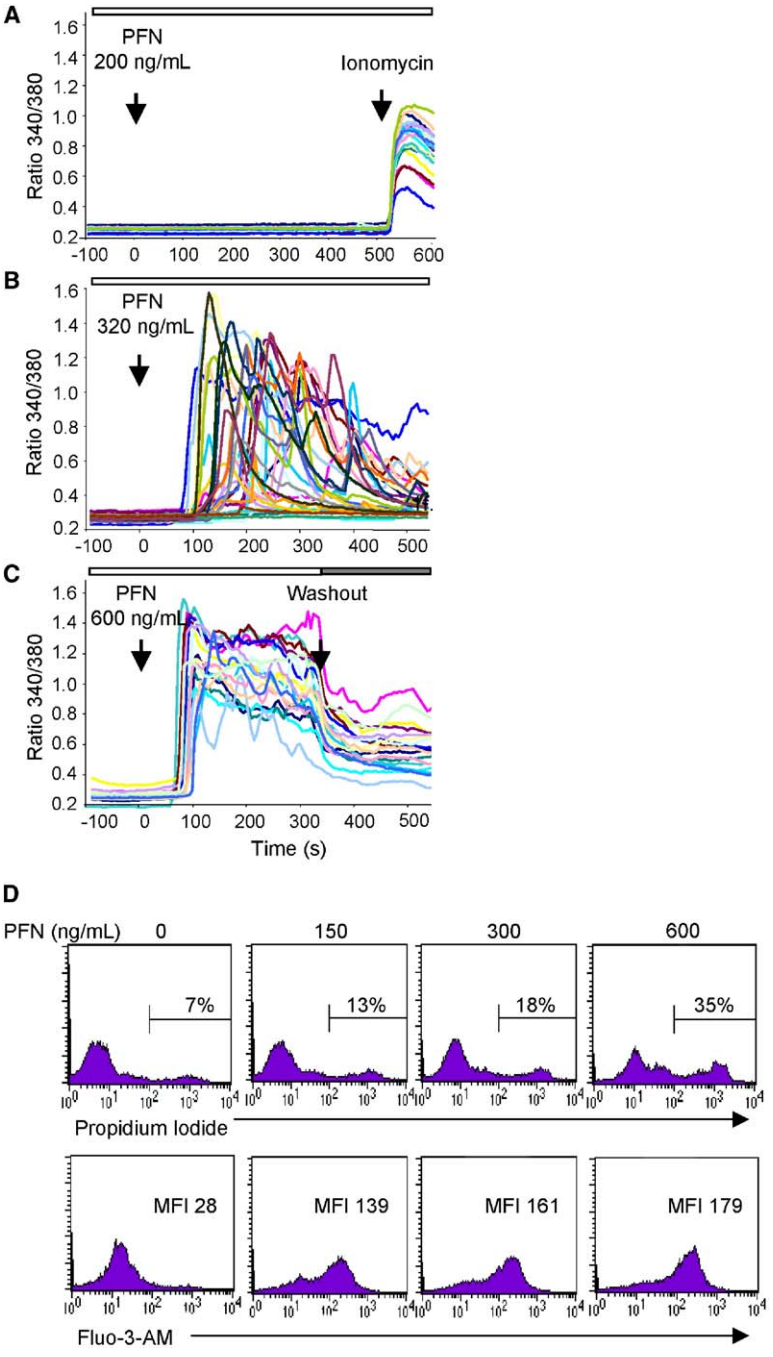

Figure 2. PFN Triggers a Ca^{2+} Flux

(A–C) Intracellular free Ca^{2+} increases following sublytic or lytic PFN treatment in HeLa cells stained with fura-2. Ca^{2+} fluxes were measured in individual cells treated at time 0 with varying PFN doses. At the lowest dose (no PI incorporation) (A), no change in Ca^{2+} was measured until ionomycin was added at 500 s. At the middle sublytic concentration (<15% PI incorporation) (B), transient Ca^{2+} fluxes were seen in all cells, while at the highest lytic dose (35% PI incorporation) (C), Ca^{2+} fluxes were sustained until extracellular calcium was removed by perfusion with calcium-free medium (gray bar). Movie S3 illustrates the Ca^{2+} fluxes in a low-power image of cells treated with sublytic PFN, while Movie S4 shows representative cells treated with a lytic concentration.

(D) Intracellular Ca^{2+} increases following PFN treatment of U937 cells stained with fluo-3 AM. Ca^{2+} concentration was measured (bottom) immediately after adding PFN. Duplicate wells were analyzed for PI incorporation (top). The lowest concentration is sublytic, while the higher concentrations are lytic.

seminate into the cytosol in most cells. Because the amount of trypan blue taken up into blebs is so small that it is difficult to visualize by microscopy, we used more sensitive fluorescent dyes (FITC-dextran, PI) to also look at uptake of small dyes into U937 cells treated with sublytic PFN by fluorescence microscopy (Figures 3C and 3D) and into cells treated with rat NK cell granules, a more physiologically relevant source of PFN, by flow cytometry (Figure 3E). In cells incubated with medium, few cells take up PI and the background mean fluorescence intensity (MFI) is ~10. However, when cells are treated with granules, the number of cells that do not stain above background for PI is reduced in a dose-dependent manner and two new populations of cells are now observed—a dimly staining (MFI ~100) and a brightly staining (MFI ~1000) population. At a lytic concentration of granules, the dim population disappears and the brightly staining cells predominate. We interpret these data to mean that the dimly staining cells have taken up the dye and contained it within blebs, while in the brightly staining cells, the membrane damage has not been controlled and dye continues to influx. Because Ca^{2+} ions diffuse much more rapidly than small dyes like trypan blue or PI, Ca^{2+} fluxes occur

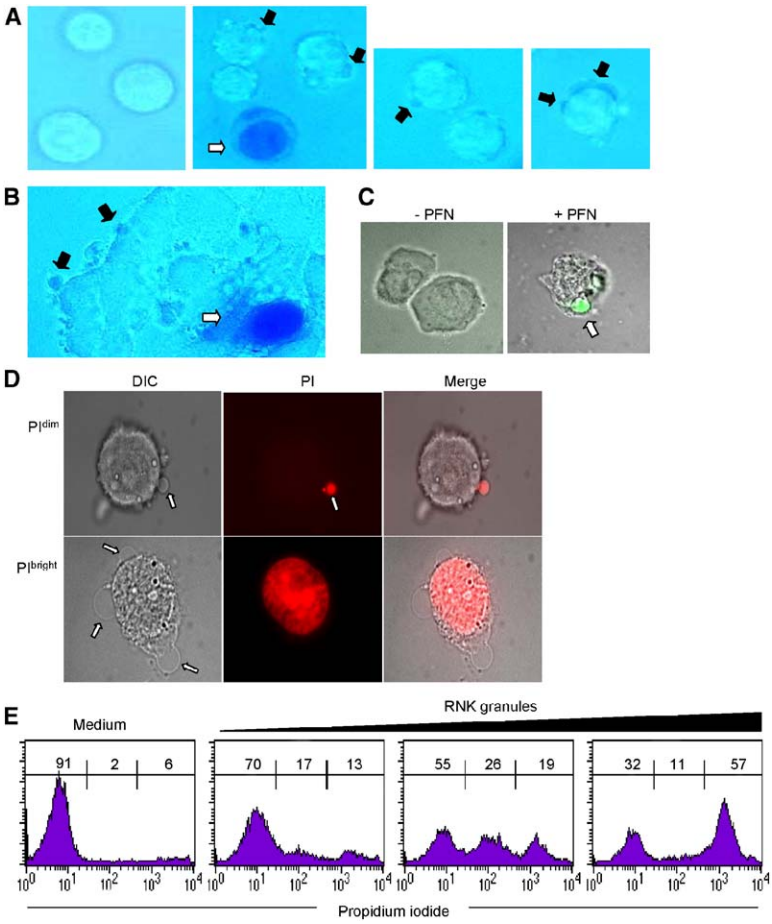

Figure 3. Small-Molecule Dyes Enter Blebs after Sublytic PFN Treatment, but Do Not Efficiently Gain Access to the Cytosol

(A and B) U937 cells (A) or HeLa cells (B) were treated with sublytic PFN in medium containing trypan blue. Trypan blue staining membrane-associated blebs (black arrows) are seen in cells that exclude trypan blue from most of the cytosol. The left panel in (A) shows control cells not exposed to PFN. In some fields, a rare necrotic cell that takes up trypan blue (white arrow) is shown for comparison.

(C and D) U937 cells treated with sublytic PFN in medium containing FITC-dextran (C) or PI (D) also take up these dyes into blebs (arrows).

(C) Merged DIC and fluorescence images.

(D) The upper cell has contained PI in a bleb, the lower cell is a rare necrotic cell in which PI is not contained and stains the nucleus. Shown are DIC (left) and fluorescence (middle) images and their merge (right).

(E) U937 cells, treated with medium or dilutions of purified RNK granules (1/150, 1/100, 1/50), were stained for PI and analyzed for PI^{dim} and PI^{bright} cells. In PI^{dim} cells, PI is likely contained in blebs.

throughout the cytosol (Figure 2), while negligible amounts of dye get into the cytosol before the membrane-limited blebs form. Because PI fluorescence is difficult to detect unless the dye is bound to nucleic acids, the detection of PI in the blebs suggests the possibility that cytosolic RNA might be in the blebs. This is consistent with an earlier, perhaps surprising, report that the apoptotic blebs produced after PFN and GzmA treatment contain RNA (Beresford et al., 1999).

PFN Triggers Lysosomal Membrane Fusion to the Plasma Membrane

When the plasma membrane is disrupted in vivo, cytosolic-free [Ca^{2+}] suddenly increases from almost undetectable levels because of high Ca^{2+} concentrations in the extracellular milieu. A stereotypic membrane-resealing response, sometimes called cellular wound healing, is rapidly triggered when cytosolic [Ca^{2+}] reaches μM concentrations. The cell responds by fusing lysosomal and other vesicular membranes to the damaged plasma membrane (McNeil and Steinhardt, 2003). Because PFN causes a Ca^{2+} flux and a Ca^{2+} flux triggers cellular-membrane resealing, we looked at whether sublytic PFN activates a process analogous to wound healing that might be responsible for maintaining membrane integrity and the transient nature of the Ca^{2+} flux. Fusion of lysosomal membranes to the damaged plasma membrane can be detected by finding the lumenal lysosomal membrane protein Lamp-1 (CD107a) on the cell surface. PFN-treated cells were costained for PI uptake and cell-surface Lamp-1. U937 cell targets were analyzed by flow cytometry (Figure 4A), and HeLa cells were examined by confocal laser scanning microscopy (Figure 4B). Diffuse uptake of small dyes, such as PI or trypan blue, indicates a sustained breach in plasma membrane integrity that correlates with necrotic death. At sublytic concentrations of 0.2–0.4 μg/ml, cells acquire cell-surface Lamp-1 expression, identified by staining without permeabilization. However, bright PI staining is seen in <10% of cells, compared to background. Other internal proteins, such as the ER-associated protein calreticulin, remain intracellular and are not detected on the cell surface. Lamp-1 can be seen in discrete patches on the cell membrane, particularly on the membrane overlying the membrane blebs (Figure 4C). This likely represents discrete fusion events of lysosomes to the plasma membrane. Blebs may form because the donated membrane causes focal increases in membrane surface area.

Since a Ca^{2+} influx is required to trigger fusion of lysosomal membranes to the plasma membrane, we determined whether Lamp-1 is externalized in cells preloaded with the cell-permeant methyl ester BAPTA-AM, which is converted within cells to the Ca^{2+} chelator

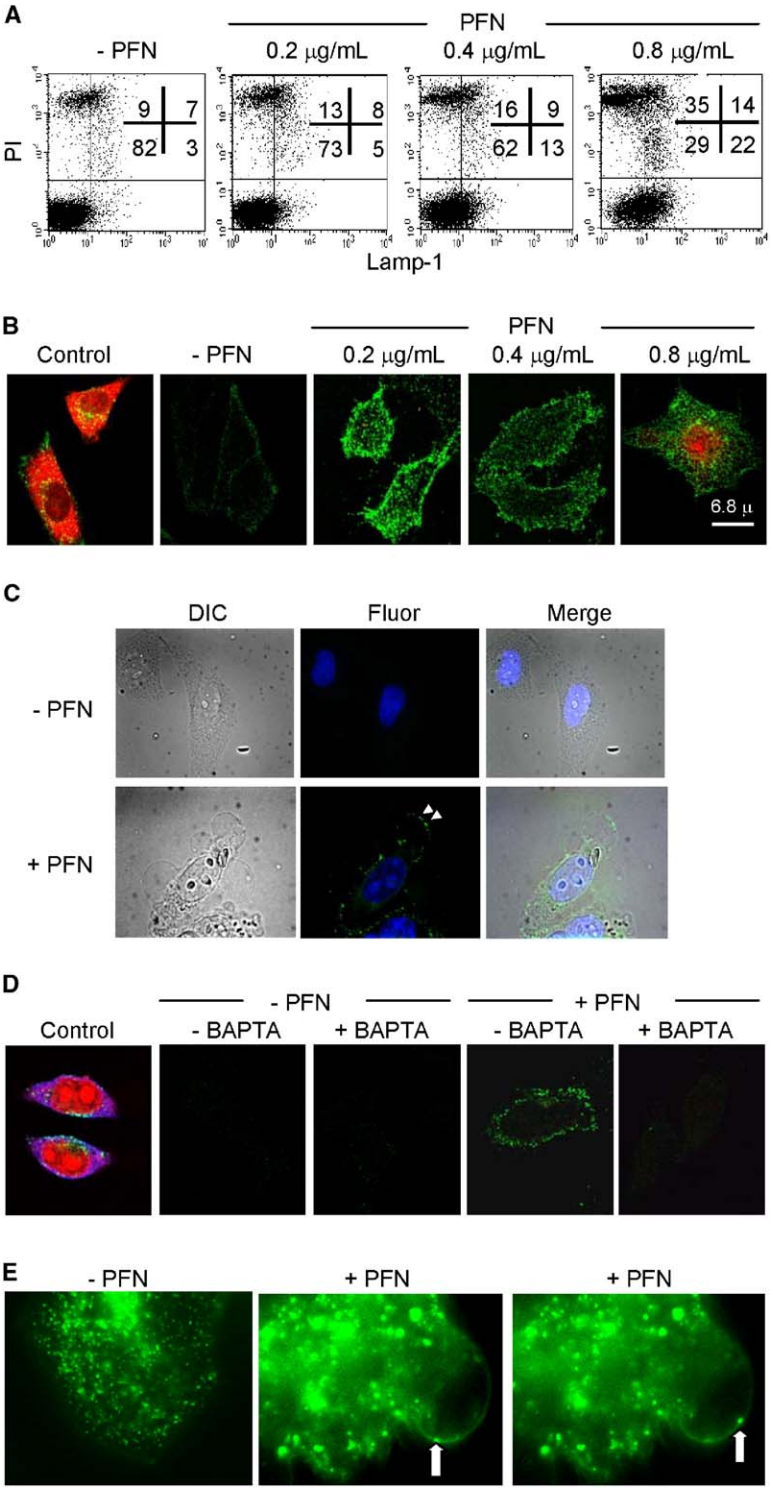

Figure 4. Sublytic PFN Triggers a Ca^{2+} Flux-Dependent Cellular Repair Response

(A and B) PFN induces a wound-healing response assessed by Lamp-1 translocation to the plasma membrane in U937 (A) and HeLa (B) cells. Cells were stained for Lamp-1 (green) and PI (red) 10 min after adding PFN. Lamp-1 accumulates on the cell surface in cells that remain impermeable to PI at lower PFN concentrations. At the highest lytic concentration, more cells become permeable to PI. Control cells, permeabilized with saponin in (B), stain for Lamp-1 (green) and PI (red).

(C) Lamp-1 cell-surface staining (green) occurs in discrete patches, particularly on blebs. Nuclei are DAPI stained (blue).

(D) Chelating intracellular Ca^{2+} by preloading cells with BAPTA-AM blocks Lamp-1 translocation. Cells were treated as in (B) with and without sublytic PFN and stained for Lamp-1, PI, and calreticulin (Alexa-647, blue). Permeabilized control cells stain for all three markers, while PFN-treated cells not loaded with BAPTA only show surface Lamp-1 staining. Single confocal sections at the cell equator are shown. BAPTA-AM treatment does not interfere with PFN activity (Figure 5).

(E) Endosomes fuse to plasma membrane at localized PFN-induced perturbations. HeLa cells, preloaded with Alexa-488-conjugated transferrin to label endosomes, were treated with sublytic PFN for 5 min, and then live cell fluorescent imaging was performed over 5 min. The left frame shows control cells not exposed to PFN. The middle and right frame show sequential still images of the same bleb at which distinct endosomes docked and fused their membranes with the plasma membrane (arrows) (Movie S5).

BAPTA (Figure 4D). BAPTA-AM treatment removes free Ca^{2+} from the cytosol but does not affect extracellular Ca^{2+}, required for PFN activity (see below). At sublytic PFN concentrations, Lamp-1 is externalized in control, but not in BAPTA-AM-loaded cells. Therefore, BAPTA-AM treatment inhibits the cellular membrane-repair response and can be used to study the effect of this target-cell repair response on PFN- and Gzm-mediated death. (Although BAPTA loading does not affect short-term cell viability, chelating intracellular Ca^{2+} may potentially interfere with other Ca^{2+}-dependent cellular processes and therefore have unanticipated confounding effects on PFN and Gzm action.)

A variety of membrane bound organelles, including

lysosomes, multivesicular bodies, and endosomes, can participate in plasma membrane resealing (McNeil and Steinhardt, 2003). To determine whether endosomes are exocytosed in response to sublytic PFN, HeLa cells were preloaded with fluorescently labeled transferrin to label endosomes, treated with PFN, and imaged by video microscopy (Figure 4E, Movie S5). Transferrin labeled the plasma membrane only of PFN-treated cells, providing evidence for PFN-triggered endosomal fusion to the plasma membrane. Fusion of transferrin-labeled endosomes selectively to the plasma membrane overlying the perturbed membrane bulges was also seen during the 5 min observation period only in cells treated with PFN (Movie S6). Therefore, both endosomes and lysosomes fuse to the plasma membrane in response to PFN. These discrete fusion events are likely responsible for the focal areas of high-intensity DiI staining in Movie S2. These results suggest that plasma membrane damage by sublytic PFN is localized and that donation of vesicular membranes only to damaged areas may account for the formation of distinct membrane blebs (Figure 1C, Movies S1, S2, and S5).

Blocking Plasma Membrane Repair by Chelating Intracellular Ca^{2+} Enhances PFN-Induced Necrosis

Because PFN multimerization and activity is Ca^{2+} dependent, we wanted to make sure that PFN activity was not compromised by chelating intracellular Ca^{2+} in cells loaded with BAPTA-AM. BAPTA loading does not affect short-term cell viability on its own or interfere with extracellular Ca^{2+}-dependent PFN-induced necrosis, assayed by PI incorporation (Figures 5A and 5B). In fact, BAPTA-loaded HeLa cells are more susceptible to PFN-mediated necrosis. While background PI incorporation in the absence of PFN was slightly different in BAPTA-loaded cells (control, 5.8% ± 0.4% versus BAPTA-AM-loaded, 7.5% ± 0.1%), at a sublytic concentration of PFN (0.2 μg/ml), there was almost twice as much cell death (control, 13.3% ± 3.4% versus BAPTA-AM-loaded, 22.6% ± 2.1%, $p < 0.02$). At a lytic concentration of PFN (0.4 μg/ml), there was also significantly more cell death (control, 29.7% ± 3.0% versus BAPTA-AM-loaded, 44.9% ± 6.7%, $p < 0.03$). At this higher concentration, the membrane-repair response could mitigate against PFN-mediated necrosis in some cells but could not patch up the damage in many cells.

A distinct dimly PI-staining population was not detected by flow cytometry in treated HeLa cells, as was seen in U937 cells in Figure 3D. Nonetheless, microscopy showed trypan blue-containing blebs in HeLa cells (Figure 3B). To look at the effect of Ca^{2+} chelation on U937 cells in which we could distinguish PI^{dim} cells, we analyzed PI incorporation in BAPTA-loaded and control cells treated with RNK granules, a more physiologically relevant reagent than purified PFN. BAPTA loading slightly increased the numbers of PI^{dim} or PI^{bright} cells in the absence of granules. After granule treatment, there was no difference in PI^{-} cells, but blocking membrane repair via Ca^{2+} chelation reduced the proportion of PI^{dim} cells from 37% ± 2% to 21% ± 1% ($p < 0.001$) and increased the necrotic PI^{bright} cells from 56% ± 2% to 72% ± 2% ($p < 0.001$). Therefore, wound healing allows the cells to avoid necrosis.

Blocking the Membrane-Repair Response Reduces PFN- and GzmB-Mediated Apoptosis

Although inhibiting membrane repair enhanced cell death, the opposite effect was observed when cells treated with sublytic PFN and GzmB were assayed for apoptosis by TUNEL staining (Figures 5D and 5E). Although there was a slight, but significant, increase in TUNEL staining of BAPTA-AM-loaded cells compared to control cells following treatment with sublytic PFN alone (control, 6.8% ± 0.3% versus BAPTA, 10.8% ± 0.9%, $p < 0.002$), there was dramatically less TUNEL staining in BAPTA-treated cells than control cells exposed to GzmB and the same amount of PFN (control, 47.5% ± 4.5% versus BAPTA, 14.9% ± 2%, $p < 0.001$). Because apoptosis is a slow process that requires ~2 hr to induce DNA damage (Shi et al., 2005), TUNEL staining was performed 2 hr after adding PFN, while necrosis was measured after 30 min. (It should be noted that during the additional incubation, some necrotic cells have already disintegrated and are not counted in the analysis.) We interpret these results to mean that if cells cannot repair the membrane damage caused by PFN, they die immediately by necrosis because the plasma membrane barrier has been irreparably breached, which precludes triggering the slower pathway of apoptosis.

PFN Triggers Rapid Endocytosis of GzmB

GzmB is taken up by target cells in the absence of PFN by endocytosis and, less efficiently, by pinocytosis (Froelich et al., 1996; Motyka et al., 2000; Pinkoski et al., 1998; Shi et al., 1997; Trapani et al., 2003; Veugelers et al., 2004). We also confirmed these findings (Shi et al., 2005). To determine whether PFN plays a role in internalizing GzmB, we incubated HeLa cells with GzmB in the presence or absence of sublytic concentrations of PFN. The uptake of GzmB is greatly accelerated and enhanced by PFN (Figure 6A). Within 2 min of adding PFN, GzmB stains prominently in large vesicles in the cytosol, while without PFN, uptake is only faintly visible above background until 10 min and staining remains weaker and is in smaller vesicles. Similar results were obtained with U937 and K562 cells (not shown). Moreover, these GzmB-containing vesicles stain for the early endosomal marker EEA-1 but not the lysosomal marker Lamp-1 (Figure 6B), suggesting that they do not arise from the membrane blebs induced by PFN. To quantify the kinetics of GzmB uptake, we used PFN to deliver GzmB fluorescently conjugated to Alexa 488 (GzmB-488 [Shi et al., 2005]) into U937 cells (Figure 6C and data not shown). By 3 min in the presence of PFN, GzmB uptake is completed. Therefore, although Gzms can be endocytosed independently of PFN, endocytosis is more efficient with PFN.

A Ca^{2+} Flux Caused by Ionomycin Does Not Activate Rapid Endocytosis of GzmB

One of the hallmarks of the membrane-repair response is to stimulate exuberant homotypic and heterotypic membrane fusion (McNeil and Steinhardt, 2003). It was therefore possible that triggering the repair response might drive rapid GzmB internalization. We thus compared the uptake of fluorescent GzmB-488 into U937

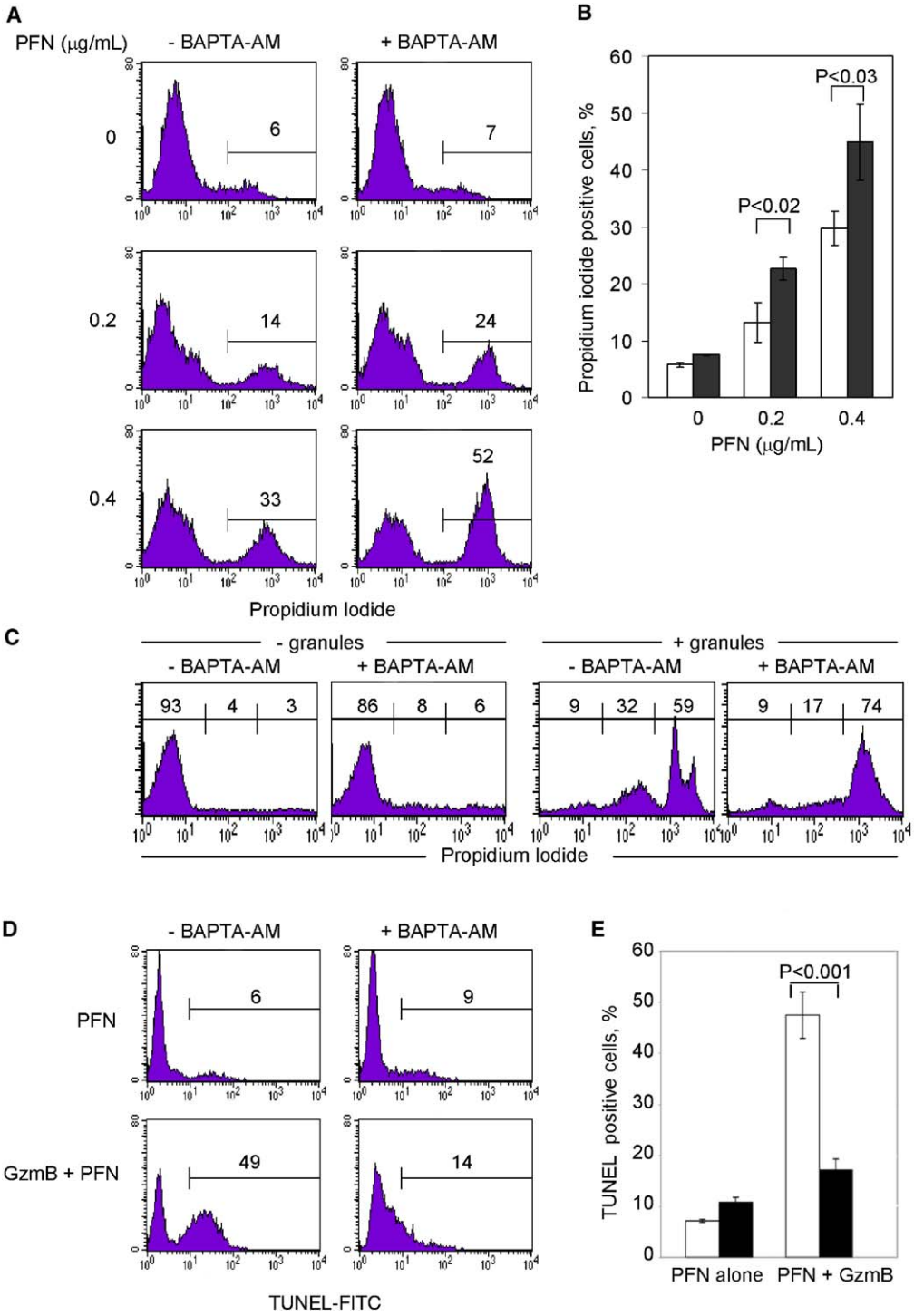

Figure 5. PFN-Induced Necrosis Is Increased in Cells Loaded with the Ca^{2+} Chelator BAPTA-AM, but GzmB-Mediated Apoptosis Is Inhibited

(A and B) Inhibiting wound healing by BAPTA-AM treatment of HeLa cells enhances PFN-induced necrosis. Plasma membrane integrity was assayed by PI incorporation 30 min after incubation at 37°C with PFN. Representative data (A) and means and SD from three independent experiments (B) are shown. White bars, untreated; black bars, BAPTA-AM treated. p values were calculated from an unpaired Student's t test.

(C) Inhibiting wound healing in U937 cells enhances PI^{bright} cells and reduces PI^{dim} cells 1 hr after treatment with RNK granules. At 1 hr, cells have not yet become apoptotic and PI^{bright} cells correspond to necrotic cells (data not shown).

(D and E) Apoptosis, assayed by TUNEL staining, is reduced in BAPTA-loaded HeLa cells treated for 2 hr with GzmB and sublytic PFN. Triplicate wells were assayed and means ± one SD are depicted in (E). Data in (D) are representative of triplicate samples from two independent experiments. White bars, untreated; black bars, BAPTA-AM treated. p values were calculated from an unpaired Student's t test. Control cells (no PFN, no GzmB) showed identical TUNEL staining as cells treated with only PFN (not shown).

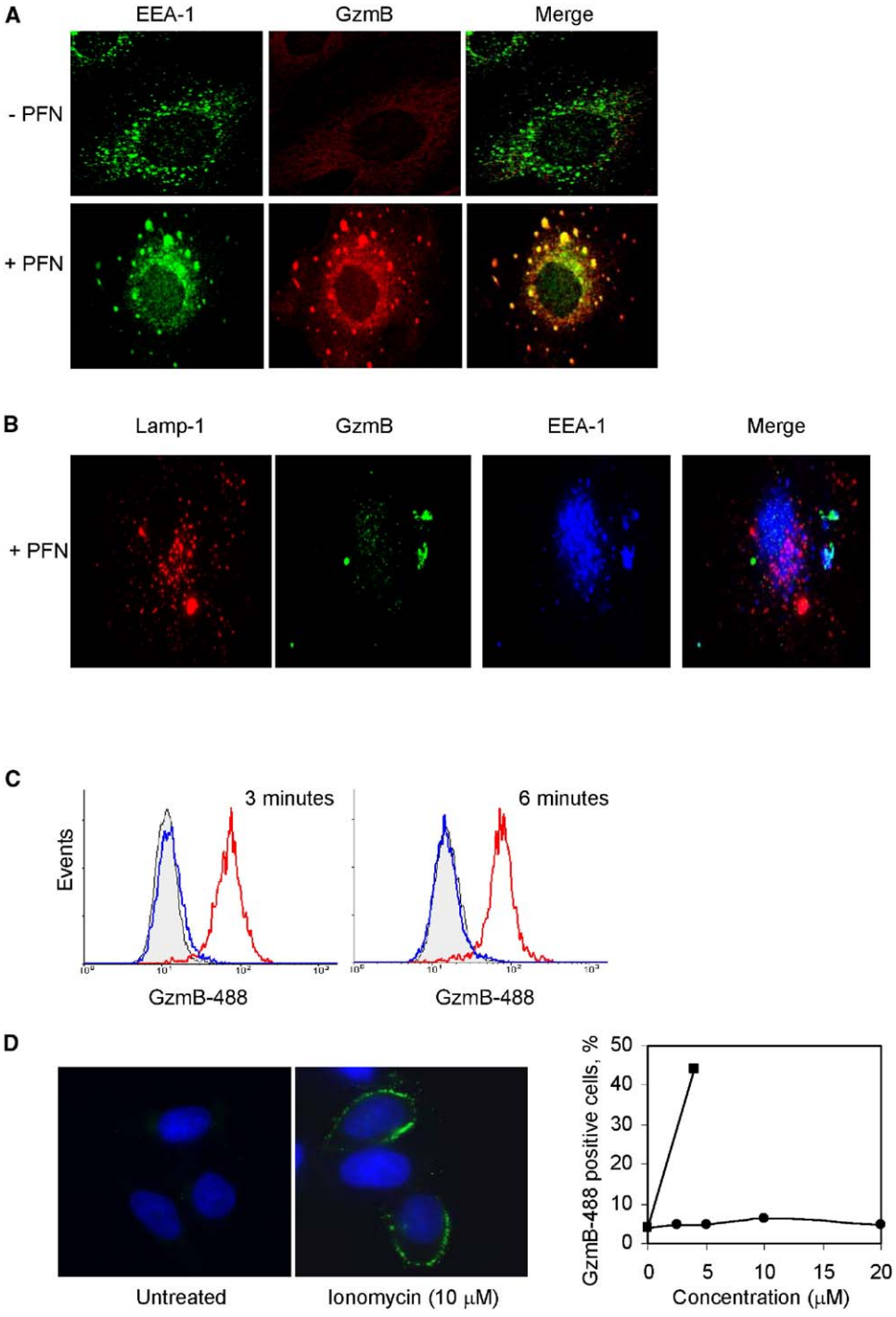

Figure 6. PFN and Ionomycin Both Induce a Cellular Membrane-Repair Response, but Only PFN Enhances GzmB Endocytosis

(A) PFN induces rapid endocytosis of GzmB by HeLa cells into large EEA-1-staining vesicles. Cells, fixed 2 min after exposure to GzmB in the presence (bottom) or absence (top) of PFN, were stained for EEA-1 and GzmB. Although some GzmB gets into cells independently of PFN, uptake is enhanced by PFN. GzmB then concentrates in atypical large EEA-1-staining vesicles.

(B) GzmB-containing vesicles stain with EEA-1 but not Lamp-1.

(C) U937 cells were loaded with GzmB-488 in the presence of sublytic PFN (red), 10 μM ionomycin (blue), or buffer (gray). PFN, but not ionomycin, causes rapid endocytosis of GzmB.

(D) Although ionomycin induces a wound-healing response assessed by Lamp-1 cell-surface staining (green; nuclei stained with DAPI [blue]), even at high sublethal concentrations of ionomycin, GzmB-488 does not enter cells. Cells were also analyzed by flow cytometry (right) for GzmB-488 uptake 10 min after treatment (ionomycin [circle], PFN [square]).

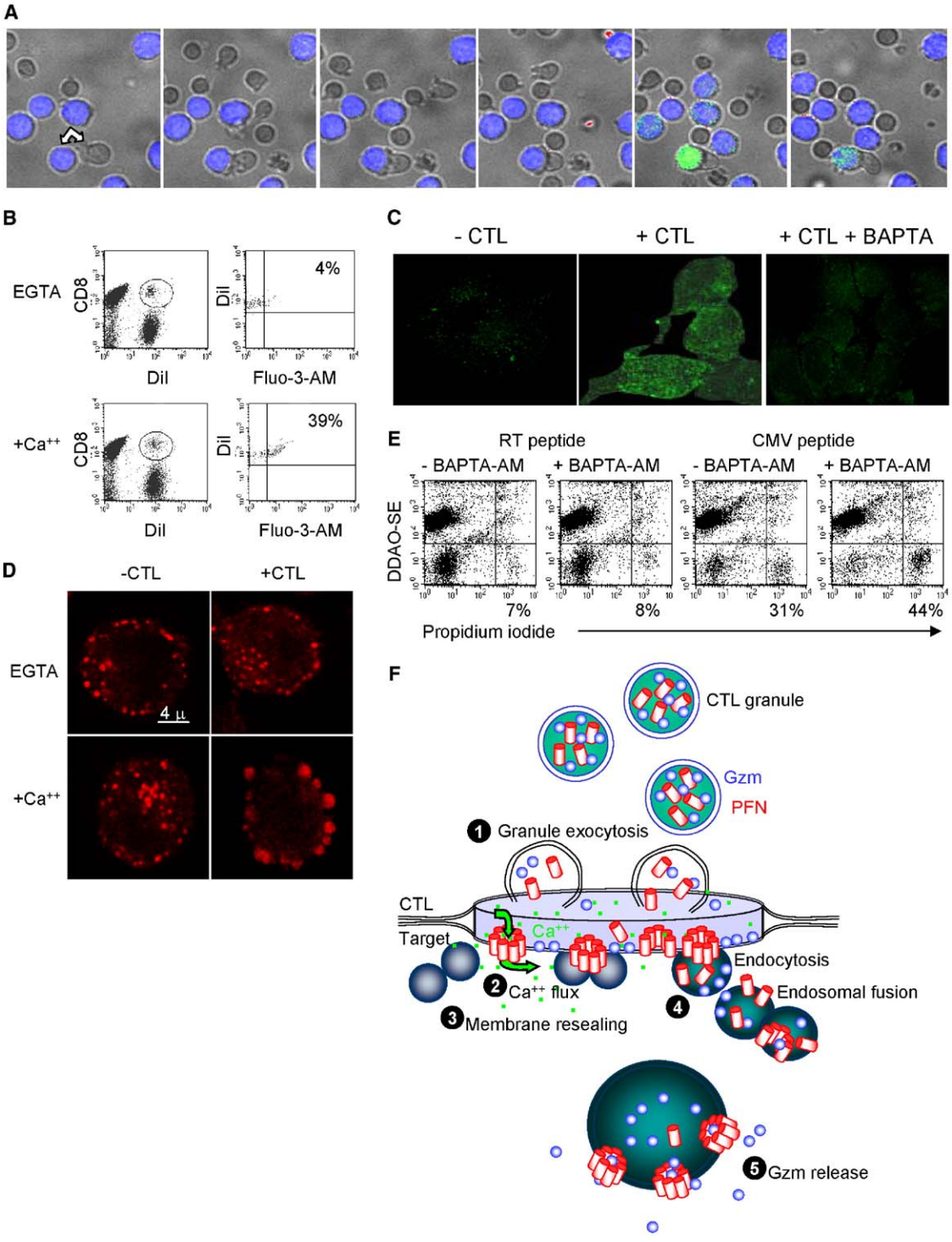

Figure 7. CTL Attack Triggers a Transient Ca^{2+} Flux and Membrane-Repair Response

(A) A PHA-activated CTL induces a transient Ca^{2+} flux (green) in a Fura-2-loaded, anti-CD3-coated U937 target cell after a firm synapse is formed between the effector and target (double arrow). Depicted are the merged DIC and fluorescent images. Approximately 30 s elapse between each frame.

(B) Intracellular Ca^{2+} increases in conA-coated K562 cells attacked by CTLs. Fluo-3-loaded K562 cells, labeled with the plasma membrane dye DiI, were spun briefly with PHA-stimulated CTLs (labeled with Cy5-conjugated anti-CD8) to induce conjugates in the absence or presence of EGTA to inhibit granule exocytosis. Fluo-3 fluorescence on gated double-positive effector:target cell conjugates indicates an increase in intracellular Ca^{2+} in the target only in the presence of extracellular Ca^{2+}. The percent of conjugates containing target cells with elevated Fluo-3 fluorescence is shown.

(C) CTL attack induces Lamp-1 (green) externalization in HeLa cell targets. ConA-coated HeLa cells were used as targets for PHA-stimulated

cells by sublytic PFN with stimulation of uptake by ionomycin. Ionomycin triggers an intracellular Ca^{2+} flux by releasing Ca^{2+} from ER stores and is also known to trigger the cellular wound healing response (Rodriguez et al., 1997). We verified this by detecting an increase in intracellular Ca^{2+} and Lamp-1 staining by confocal laser scanning microscopy on unpermeabilized HeLa cells treated with ionomycin (Figure 6D, data not shown). However, although it triggers cellular wound healing, ionomycin does not enhance GzmB-488 uptake by U937 cells, even at the highest concentrations that do not cause cell death (Figures 6C and 6D). Therefore, PFN likely needs to do more than trigger a Ca^{2+} flux and wound healing to cause rapid GzmB endocytosis.

Cytotoxic T Lymphocytes Trigger a Ca^{2+} Flux and Membrane-Repair Response in Target Cells

Although treating cells with GzmB and sublytic PFN is a good model to study the steps of apoptosis induction by CTL, it may not faithfully replicate what happens when a killer cell destroys a target cell, where PFN and granzymes are delivered in the spatially limited region of the immunological synapse. To determine whether the Ca^{2+} flux and membrane-repair response observed after loading cells with PFN is physiologically relevant, we looked for changes in intracellular Ca^{2+} and Lamp-1 externalization in target cells subjected to attack by phytohemagglutinin (PHA)-activated human CTL. U937 cells coated with anti-CD3 and preloaded with the Ca^{2+} indicator dye fura-2 were incubated with CTL and visualized by digital interference contrast (DIC) and fluorescence microscopy. Within a few minutes of forming a firm synapse between the CTL and its target, a transient target-cell Ca^{2+} flux was seen (Figure 7A) Similar results were found by flow cytometry gating on CTL:target conjugates using concanavalin A (conA)-coated, Fluo-3-AM-loaded K562 targets incubated with the same effector cells (Figure 7B). Control experiments performed with medium containing EGTA showed almost no target-cell Ca^{2+} flux. After CTL attack, target cells also exhibit the hallmark feature of the plasma membrane-repair response, cell-surface Lamp-1 staining (Figure 7C). As expected, Lamp-1 externalization is inhibited by BAPTA-AM treatment of target cells (Figure 7C). These results show that wound healing also occurs in target cells subjected to CTL attack. When concanavalin A-coated HeLa cells are subjected to CTL attack, we also detect large EEA-1-staining membrane-proximal vesicles that resemble the EEA-1-staining GzmB-containing vesicles seen during PFN loading of GzmB in Figure 6A (Figure 7D). Moreover, just as inhibiting wound healing in PFN or granule-loading experiments enhances target-cell necrosis and inhibits apoptosis, inhibiting wound healing using BAPTA-AM during CTL attack also promotes necrosis. If CMV peptide-coated B cell targets are loaded with BAPTA-AM before initiating attack by CMV-specific CTLs, necrotic cell death, assayed by PI^{bright} staining 1 hr later (before apoptosis has occurred), is significantly enhanced (representative flow cytometry data, Figure 7E). Although PI^{bright} staining of CTL-exposed target cells incubated with an irrelevant peptide is not changed by BAPTA-AM treatment (8% ± 1% both with and without BAPTA-AM), PI^{bright} cells are increased over background from 27% ± 4% to 35% ± 3% ($p < 0.0001$) in BAPTA-AM-loaded target cells. Although the difference is small (a 27% increase in necrosis over background), these data were reproduced in two additional independent experiments. Therefore, the wound-healing response in target cells subjected to CTL attack contributes to preventing necrosis, recapitulating our results obtained with sublytic PFN or isolated NK cell granules.

Discussion

In this study, we reexamined the effect of native PFN on the target-cell membrane. At sublytic concentrations that do not cause cell death on their own, PFN damages the plasma membrane and induces a transient Ca^{2+} flux, which triggers a cellular repair response, reminiscent of the cellular wound-healing response that reseals holes in injured cell membranes using pieces of membranes donated by intracellular organelles. Cells treated with sublytic PFN take up small amounts of fluid phase dyes, suggesting that at least small pores are formed at the plasma membrane. These pores probably cause an influx of Ca^{2+} from the Ca^{2+}-rich extracellular milieu to the Ca^{2+}-poor cytosol. However, fluid phase dyes do not distribute throughout the cytosol, but remain localized near the plasma membrane in membrane bound blebs. At the same time, the Ca^{2+} flux is transient. This likely reflects a wound-heal-

CTLs. Pretreating the targets with BAPTA-AM inhibits the repair response to CTL attack. Cells were stained without permeabilization or fixation. Representative projected Z stack series are shown. CTLs are absent from these images, as nonadherent cells wash off during staining.

(D) ConA-coated HeLa cells subjected to CTL attack for 2 min develop large EEA-1-staining membrane-proximal vesicles similar to those detected following PFN loading.

(E) Blocking wound healing by chelating Ca^{2+} enhances the proportion of necrotic PI^{bright} target cells 1 hr after initiating attack by CMV-specific CTLs. In this experiment, CTL were labeled with DDAO-SE dye, and the proportion of $DDAO\text{-}SE^{-}$ B cell targets that stain brightly with PI are shown. Data are representative of quadruplicate samples. Numbers indicate the proportion of PI^{bright} $DDAO\text{-}SE^{-}$ target cells. There was no increase in PI^{bright} target cells incubated with an irrelevant HIV reverse transcriptase (RT) peptide after BAPTA treatment.

(F) Model for PFN delivery of Gzms. After CTL granule exocytosis into the immunological synapse (1), PFN multimerizes in the target-cell membrane to form pores through which Ca^{2+} and small molecule dyes enter (2), triggering a plasma membrane repair response (3) in which endosomes and lysosomes fuse with the damaged plasma membrane to reseal it. The fusion produces membrane bound blebs, some of which may be shed from the cell. PFN also triggers the rapid endocytosis (4) of PFN and Gzms into large endosomes, which may be formed in part by rapid homotypic fusion of endosomes, in response to the transient Ca^{2+} flux. We hypothesize that PFN then forms pores in the endosome membrane, releasing Gzms into the target-cell cytoplasm (5), where they initiate programmed cell death. The model for Gzm delivery in steps (4) and (5) requires experimental verification.

ing response, which walls off the damaged membrane and seals the cytosol. During CTL or NK cell death, the restoration of plasma membrane integrity by the plasma membrane-repair response protects the cell from necrosis and allows the Gzms to trigger the slower process of apoptosis. Since necrotic cells cause an inflammatory response while apoptotic cells are recognized and phagocytosed rapidly with less inflammation, this allows the immune response to maintain its specificity for targeted cells, minimizing bystander cell damage (Huynh et al., 2002). At lytic PFN concentrations, the repair response cannot keep up with membrane damage, the pores are not sealed, and the plasma membrane barrier is lethally disrupted. However, since cells targeted by granule-mediated cytolysis die by apoptosis (Russell et al., 1980), the sublytic concentration is the physiologically relevant one.

Balaji et al. recently proposed a mechanism by which CTLs protect themselves from membrane damage by PFN (Balaji et al., 2002). According to their model, membrane-associated cathepsin B on the lumenal surface of CTL granules relocalizes to the CTL plasma membrane during cytotoxic granule exocytosis and cleaves and inactivates any PFN redirected back toward the killer cell. Since cathepsin B is also on the membrane of lysosomes, a similar mechanism may be operating following wound healing to limit continued target-cell membrane damage by PFN.

Many of the results in this study were obtained by treating target cells with native PFN. However, this is an imperfect surrogate for what happens during targeted delivery of PFN and Gzms by killer cells into the immunological synapse. The local PFN concentration at the synapse may be higher than what is optimal for loading by sublytic PFN. We were therefore careful to validate our results by looking at what happens during CTL attack. During CTL attack, we detected a transient Ca^{2+} flux and membrane-repair response with characteristic Lamp-1 externalization in target cells and appearance of large EEA-1-staining vesicles (Figure 7). Moreover, the repair response and target-cell apoptosis were inhibited by chelating intracellular Ca^{2+}.

Experiments to decipher the mechanism of PFN action are tricky because of the narrow window for PFN to deliver Gzms to induce apoptosis, where a 3- to 4-fold difference separates a subthreshold dose for delivering Gzms and a necrotic dose. Measuring the Ca^{2+} flux is a good way to monitor the effective concentration of PFN for loading Gzms. If there is no Ca^{2+} flux, the concentration is too low to deliver Gzms; if the flux is transient, the concentration is sublytic; if the flux is sustained, the cells are killed by necrosis and the concentration is too high. A molecular understanding of how PFN induces a Ca^{2+} flux is still needed, but likely depends on the demonstrated ability of PFN to insert into membranes and multimerize in a Ca^{2+}-dependent manner to form membrane pores (Masson and Tschopp, 1985; Millard et al., 1984; Sauer et al., 1991; Young et al., 1986). The existence of pores is verified by the entry of small molecule dyes into submembrane blebs. These pores are unlikely to be large enough to allow Gzms into the cell, since the Gzms are initially found within EEA-1-staining large vesicles, rather than disseminated throughout the cytoplasm. It is also unlikely that the large GzmA-containing vesicles arise from the blebs formed during the repair process, since the repair process inserts Lamp-1 into the plasma membrane, but the Gzm-containing vesicles do not stain with Lamp-1.

Therefore, we favor a model (Figure 7F) in which PFN triggers rapid endocytosis, which causes basic Gzms, bound to negatively charged glycosaminoglycans on the plasma membrane by charge (Kurschus et al., 2004; Shi et al., 2005), to be internalized into endosomes. These endosomes may fuse with one another because of the exuberant homotypic and heterotypic membrane fusion characteristic of the membrane-repair response (McNeil and Steinhardt, 2003) to form the large EEA-1-staining vesicles seen within a minute or two of adding PFN to cells or triggering CTL attack. Membrane fusion events likely are also responsible for the membrane bubbling and intracellular connections seen after treatment with sublytic PFN. Endocytosis is just the first step of PFN delivery of Gzms to the cytosol. Within ~10 min of PFN treatment, these large vesicles, which also stain for PFN, disappear, and Gzms are disseminated throughout the cell (D.K., L.S., S.F., F.N., R.M., T.K., and J.L., unpublished data). We hypothesize that PFN within these vesicles damages the vesicular membrane to form large pores that release Gzms into the cytosol where they activate apoptosis. However, this piece of the model requires experimental validation.

PFN facilitates the rapid uptake of GzmB (Figure 6) into EEA-1-staining vesicles. Although Gzms are endocytosed without PFN (Froelich et al., 1996), this process is inefficient and unlikely to be physiologically relevant during CTL attack when PFN-mediated delivery is completed within a few minutes. A recent study using cells expressing dominant-negative mutant dynamin suggests that dynamin-dependent endocytosis is required to trigger GzmB- and PFN-mediated apoptosis (Veugelers et al., 2004). We confirmed this finding (D.K., L.S., S.F., F.N., R.M., T.K., and J.L., unpublished data). However, another study that looked only at cell death did not find dynamin to be important (Trapani et al., 2003). One way to reconcile these seemingly contradictory data would be if dynamin were not required for necrotic death by PFN since it involves direct plasma membrane damage, while dynamin-dependent endocytosis is needed for PFN to deliver Gzms to activate apoptosis. Because the difference between lytic and sublytic PFN concentration is so small and the activity of stored PFN is not very stable, special care is required in doing experiments with PFN to distinguish between its necrotic and Gzm delivery functions.

The membrane-repair response may not be responsible for the rapid PFN-mediated endocytosis of Gzms, since ionomycin, another stimulus for the repair response, does not enhance GzmB internalization. However, because ionomycin persists in treated cells, causing sustained increases in intracellular Ca^{2+}, while generally after PFN treatment or membrane resealing the Ca^{2+} flux is transient, this question needs to be examined using other initiators of membrane damage. The molecular basis for PFN-mediated delivery of Gzms into the large endocytic vesicles and from there to the cytosol still needs to be understood. This study suggests that although both the original pore model and the revised pore-independent endosomolysis model

for PFN action may be correct in certain respects, neither fully explains all of the data. Our revised model, which incorporates some features of both models, is consistent with the known data.

The target cell is therefore an active participant in its own death. The membrane-repair response allows the target to restore membrane integrity, avoid necrosis, and undergo apoptosis. Because apoptotic, but not necrotic, cells are rapidly phagocytosed, target-cell membrane repair should reduce inflammation caused by necrotic cells. This should help maintain immune specificity, eliminating the intended target cell without causing harm to bystander cells.

Experimental Procedures

Cell Lines and Reagents

U937 cells were grown in cell-culture medium (RPMI 1640 supplemented with 10% FCS, 2 mM glutamine, 2 mM HEPES, 100 U/ml penicillin, 100 mg/ml streptomycin, and 50 μM β-mercaptoethanol). HeLa cells were grown to roughly 60% confluency in DMEM, supplemented as above, on collagen-coated BIOCOAT slides (BD Labware, Beverly, MA). CTLs were generated from human PBMCs treated with 2 μg/ml PHA and cultured for 7–20 days in cell-culture medium containing 600 IU/ml recombinant human IL-2 (a kind gift of Chiron Oncology). In some experiments, CMV peptide-specific CTL, generated as described (Martinvalet et al., 2005), was used to lyse autologous EBV-transformed B cells, pulsed with specific CMV peptide or control peptide. Cytotoxic granules, GzmB, and PFN were purified from rat NK cells as described (Shi et al., 2000). Recombinant GzmB was purified from baculovirus as reported (Xia et al., 1998). Rabbit anti-GzmB was produced in the laboratory of the late A. Greenberg (University of Winnipeg) and has been described (Shi et al., 2000). Mouse Lamp-1 mAb was from Developmental Studies Hybridoma Bank (University of Iowa); goat anti-EEA-1 was from Santa Cruz; rabbit anti-calreticulin was from Stressgen Biotechnology; Cy5-conjugated anti-CD8 was from Caltag; and anti-CD3 was purified from the OKT3 hybridoma. ConA and PI were from Sigma. AlexaFluor 488 (Molecular Probes) was used to label recombinant GzmB using the manufacturer's protocol. Sytox green, DiI, FITC-dextran, BAPTA-AM, fluo-3-AM, fura-2-AM, DDAO-SE, Alexa-488 conjugated transferrin, and Alexa-conjugated secondary antibodies were from Molecular Probes.

PFN and GzmB Loading

Cells were equilibrated in cell-loading buffer (HBSS with 10 mM HEPES, 2 mM $CaCl_2$, 0.4% BSA). PFN and/or GzmB were added simultaneously at the indicated doses for the indicated times. The sublytic PFN dose was determined independently for each cell line, PFN preparation and experiment, as the concentration required to induce 5%–15% trypan blue or PI uptake (Shi et al., 1992). PI (final concentration, 2 μg/ml) was added during or after PFN incubation where indicated. For apoptosis assays, cells were incubated for 4 hr at 37°C. For GzmB-488 uptake assays, U937 or HeLa cells were incubated for the indicated times with GzmB-488 (30 μg/ml) in the presence of cell-loading buffer alone, 10 μM ionomycin, or PFN (0.1 μg/ml or indicated concentrations for U937; 0.4 μg/ml for HeLa). U937 cells were washed in 1 mM 5 kDa dextran sulfate to remove surface bound GzmB before flow cytometry as described (Shi et al., 2005).

Supplemental Data

Supplemental Data include six movies and Supplemental Experimental Procedures and can be found with this article online at http://www.immunity.com/cgi/content/full/23/3/249/DC1/.

Acknowledgments

This work was supported by NIH Grants R01 AI45587 (J.L.), U54 AI57159 (T.K.), PO1 HL59561 (T.K.), R21 AI54933 (S.F.), and T32 HL066987 (D.K.), and a research grant from the Immune Deficiency Foundation (S.F.). The Perkin Fund provided support for some of the imaging equipment. Several of the reagents used for this work (rat NK granules and native GzmB) were prepared in the laboratory of the late A. Greenberg (Manitoba Institute of Cell Biology, Winnipeg, Canada).

Received: March 29, 2005
Revised: July 8, 2005
Accepted: July 19, 2005
Published: September 19, 2005

References

Balaji, K.N., Schaschke, N., Machleidt, W., Catalfamo, M., and Henkart, P.A. (2002). Surface cathepsin B protects cytotoxic lymphocytes from self-destruction after degranulation. J. Exp. Med. *196*, 493–503.

Beresford, P.J., Xia, Z., Greenberg, A.H., and Lieberman, J. (1999). Granzyme A loading induces rapid cytolysis and a novel form of DNA damage independently of caspase activation. Immunity *10*, 585–594.

Bi, G.Q., Alderton, J.M., and Steinhardt, R.A. (1995). Calcium-regulated exocytosis is required for cell membrane resealing. J. Cell Biol. *131*, 1747–1758.

Binah, O., Liu, C.C., Young, J.D., and Berke, G. (1997). Channel formation and [Ca2+]i accumulation induced by perforin N-terminus peptides: comparison with purified perforin and whole lytic granules. Biochem. Biophys. Res. Commun. *240*, 647–650.

Browne, K.A., Blink, E., Sutton, V.R., Froelich, C.J., Jans, D.A., and Trapani, J.A. (1999). Cytosolic delivery of granzyme B by bacterial toxins: evidence that endosomal disruption, in addition to transmembrane pore formation, is an important function of perforin. Mol. Cell. Biol. *19*, 8604–8615.

Catalfamo, M., and Henkart, P.A. (2003). Perforin and the granule exocytosis cytotoxicity pathway. Curr. Opin. Immunol. *15*, 522–527.

Froelich, C.J., Orth, K., Turbov, J., Seth, P., Gottlieb, R., Babior, B., Shah, G.M., Bleackley, R.C., Dixit, V.M., and Hanna, W. (1996). New paradigm for lymphocyte granule-mediated cytotoxicity. J. Biol. Chem. *271*, 29073–29079.

Huynh, M.L., Fadok, V.A., and Henson, P.M. (2002). Phosphatidylserine-dependent ingestion of apoptotic cells promotes TGF-beta1 secretion and the resolution of inflammation. J. Clin. Invest. *109*, 41–50.

Kagi, D., Ledermann, B., Burki, K., Seiler, P., Odermatt, B., Olsen, K.J., Podack, E.R., Zinkernagel, R.M., and Hengartner, H. (1994). Cytotoxicity mediated by T cells and natural killer cells is greatly impaired in perforin-deficient mice. Nature *369*, 31–37.

Kawasaki, Y., Saito, T., Shirota-Someya, Y., Ikegami, Y., Komano, H., Lee, M.H., Froelich, C.J., Shinohara, N., and Takayama, H. (2000). Cell death-associated translocation of plasma membrane components induced by CTL. J. Immunol. *164*, 4641–4648.

Kurschus, F.C., Kleinschmidt, M., Fellows, E., Dornmair, K., Rudolph, R., Lilie, H., and Jenne, D.E. (2004). Killing of target cells by redirected granzyme B in the absence of perforin. FEBS Lett. *562*, 87–92.

Lieberman, J. (2003). Cell death and immunity: the ABCs of granule-mediated cytotoxicity: new weapons in the arsenal. Nat. Rev. Immunol. *3*, 361–370.

Martinvalet, D., Zhu, P., and Lieberman, J. (2005). Granzyme A induces caspase-independent mitochondrial damage, a required first step for apoptosis. Immunity *22*, 355–370.

Masson, D., and Tschopp, J. (1985). Isolation of a lytic pore forming protein (perforin) from cytolytic T cells. J. Biol. Chem. *260*, 9069–9073.

McNeil, P.L., and Steinhardt, R.A. (2003). Plasma membrane disruption: repair, prevention, adaptation. Annu. Rev. Cell Dev. Biol. *19*, 697–731.

Metkar, S.S., Wang, B., Aguilar-Santelises, M., Raja, S.M., Uhlin-Hansen, L., Podack, E., Trapani, J.A., and Froelich, C.J. (2002). Cytotoxic cell granule-mediated apoptosis: perforin delivers gran-

zyme B-serglycin complexes into target cells without plasma membrane pore formation. Immunity *16*, 417–428.

Millard, P.J., Henkart, M.P., Reynolds, C.W., and Henkart, P.A. (1984). Purification and properties of cytoplasmic granules from cytotoxic rat LGL tumors. J. Immunol. *132*, 3197–3204.

Miyake, K., and McNeil, P.L. (1995). Vesicle accumulation and exocytosis at sites of plasma membrane disruption. J. Cell Biol. *131*, 1737–1745.

Motyka, B., Korbutt, G., Pinkoski, M.J., Heibein, J.A., Caputo, A., Hobman, M., Barry, M., Shostak, I., Sawchuk, T., Holmes, C.F., et al. (2000). Mannose 6-phosphate/insulin-like growth factor II receptor is a death receptor for granzyme B during cytotoxic T cell-induced apoptosis. Cell *103*, 491–500.

Pinkoski, M.J., Hobman, M., Heibein, J.A., Tomaselli, K., Li, F., Seth, P., Froelich, C.J., and Bleackley, R.C. (1998). Entry and trafficking of granzyme B in target cells during granzyme B-perforin-mediated apoptosis. Blood *92*, 1044–1054.

Podack, E.R., Young, J.D.-E., and Cohn, Z.A. (1985). Isolation and biochemical and functional characterization of perforin 1 from cytolytic T cell granules. Proc. Natl. Acad. Sci. USA *82*, 8629–8633.

Poenie, M., Tsien, R.Y., and Schmitt-Verhulst, A.M. (1987). Sequential activation and lethal hit measured by [Ca2+]i in individual cytolytic T cells and targets. EMBO J. *6*, 2223–2232.

Reddy, A., Caler, E.V., and Andrews, N.W. (2001). Plasma membrane repair is mediated by Ca(2+)-regulated exocytosis of lysosomes. Cell *106*, 157–169.

Rodriguez, A., Webster, P., Ortego, J., and Andrews, N.W. (1997). Lysosomes behave as Ca2+-regulated exocytic vesicles in fibroblasts and epithelial cells. J. Cell Biol. *137*, 93–104.

Russell, J.H., Masakowski, V.R., and Dobos, C.B. (1980). Mechanisms of immune lysis. I. Physiological distinction between target cell death mediated by cytotoxic T lymphocytes and antibody plus complement. J. Immunol. *124*, 1100–1105.

Sauer, H., Pratsch, L., Tschopp, J., Bhakdi, S., and Peters, R. (1991). Functional size of complement and perforin pores compared by confocal laser scanning microscopy and fluorescence microphotolysis. Biochim. Biophys. Acta *1063*, 137–146.

Shi, L., Kraut, R.P., Aebersold, R., and Greenberg, A.H. (1992). A natural killer cell granule protein that induces DNA fragmentation and apoptosis. J. Exp. Med. *175*, 553–566.

Shi, L., Mai, S., Israels, S., Browne, K., Trapani, J.A., and Greenberg, A.H. (1997). Granzyme B (GraB) autonomously crosses the cell membrane and perforin initiates apoptosis and GraB nuclear localization. J. Exp. Med. *185*, 855–866.

Shi, L., Yang, X., Froelich, C.J., and Greenberg, A.H. (2000). Purification and use of granzyme B. Methods Enzymol. *322*, 125–143.

Shi, L., Keefe, D., Durand, E., Feng, H., Zhang, D., and Lieberman, J. (2005). Granzyme B binds to target cells mostly by charge and must be added at the same time as perforin to trigger apoptosis. J. Immunol. *174*, 5456–5461.

Steinhardt, R.A., Bi, G., and Alderton, J.M. (1994). Cell membrane resealing by a vesicular mechanism similar to neurotransmitter release. Science *263*, 390–393.

Stepp, S.E., Dufourcq-Lagelouse, R., Le Deist, F., Bhawan, S., Certain, S., Mathew, P.A., Henter, J.I., Bennett, M., Fischer, A., de Saint Basile, G., and Kumar, V. (1999). Perforin gene defects in familial hemophagocytic lymphohistiocytosis. Science *286*, 1957–1959.

Stinchcombe, J.C., Bossi, G., Booth, S., and Griffiths, G.M. (2001). The immunological synapse of CTL contains a secretory domain and membrane bridges. Immunity *15*, 751–761.

Trapani, J.A., Sutton, V.R., Thia, K.Y., Li, Y.Q., Froelich, C.J., Jans, D.A., Sandrin, M.S., and Browne, K.A. (2003). A clathrin/dynamin- and mannose-6-phosphate receptor-independent pathway for granzyme B-induced cell death. J. Cell Biol. *160*, 223–233.

Tschopp, J., Masson, D., and Stanley, K.K. (1986). Structural/functional similarity between proteins involved in complement- and cytotoxic T-lymphocyte-mediated cytolysis. Nature *322*, 831–834.

Veugelers, K., Motyka, B., Frantz, C., Shostak, I., Sawchuk, T., and Bleackley, R.C. (2004). The granzyme B-serglycin complex from cytotoxic granules requires dynamin for endocytosis. Blood *103*, 3845–3853.

Xia, Z., Kam, C.M., Huang, C., Powers, J.C., Mandle, R.J., Stevens, R.L., and Lieberman, J. (1998). Expression and purification of enzymatically active recombinant granzyme B in a baculovirus system. Biochem. Biophys. Res. Commun. *243*, 384–389.

Young, J.D., Nathan, C.F., Podack, E.R., Palladino, M.A., and Cohn, Z.A. (1986). Functional channel formation associated with cytotoxic T-cell granules. Proc. Natl. Acad. Sci. USA *83*, 150–154.